

Computer Simulation of Particle Overlap in Fiber Count Samples

Chih-Chieh Chen , Tai-Shan Yu , Tung-Sheng Shih & Paul Baron

To cite this article: Chih-Chieh Chen , Tai-Shan Yu , Tung-Sheng Shih & Paul Baron (2001) Computer Simulation of Particle Overlap in Fiber Count Samples, AIHAJ - American Industrial Hygiene Association, 62:3, 281-287, DOI: [10.1080/15298660108984629](https://doi.org/10.1080/15298660108984629)

To link to this article: <https://doi.org/10.1080/15298660108984629>



Published online: 04 Jun 2010.



Submit your article to this journal [↗](#)



Article views: 21

Computer Simulation of Particle Overlap in Fiber Count Samples

AUTHORS

Chih-Chieh Chen^a
 Tai-Shan Yu^a
 Tung-Sheng Shih^b
 Paul Baron^c

^aInstitute of Occupational Medicine and Industrial Hygiene, College of Public Health, National Taiwan University, 1 Jen-Ai Rd., Sec. 1, Taipei, Taiwan;

^bInstitute of Occupational Safety and Health, Council of Labor Affairs, Taipei, Taiwan;

^cNational Institute for Occupational Safety and Health Cincinnati, OH

Fibrous aerosols are of great importance to industrial hygienists because of the severe health risks that may be associated with inhaling such particles. Previous studies on measurement error due to overloading of fibers and nonfibrous particles on the collected sample indicate that a 100–1300 fiber/mm² filter area is the best filter loading density to reduce bias in fiber counts. The present study investigated the upper fiber and particle concentration limits for reliable counting and identification and the possibility of a procedure for correcting observed fiber counts to account for fiber masking due to overlapping particles or fibers. A computer-generated grid was used to simulate the light microscope graticule field. The resolution of 2000 × 2000 was found to accurately represent the shape of the fibers and nonfibrous particles. Bivariate lognormal distributions were used to describe the length and width distributions of the fibers. The capability of distinguishing particle-overlapped fibers (defined as the resolution index), the coverage of the graticule field, the filter surface loading density, size distributions of fibers and particles, and the fiber-to-particle concentration ratio were the primary parameters in this study. The counting efficiency was found to consistently decrease with increasing filter surface loading density and decreasing resolution index. The recommended upper limit of filter surface fiber density depended not only on the number concentration ratio but also on the filter surface loading densities and size distributions of fibers and particles. The advantage of using a thoracic preseparator on counting efficiency was calculated and found to improve counting efficiency significantly when the count median diameter of nonfibrous particles was close to or larger than the thoracic 50% cutoff point of 10 μm.

Keywords: fiber counting, fibrous aerosols, thoracic preseparator

The National Institute for Occupational Safety and Health (NIOSH) Method 7400⁽¹⁾ is a fiber counting method used to estimate asbestos exposure in the workplace and to determine cleanliness after asbestos abatement in schools and other buildings.⁽²⁾ Filter collection of the fibers is followed by phase contrast microscope analysis, in which fibers are observed and counted on an optically clear filter. The ability of the analyst to distinguish the fibers from the background and other particles is an important factor in the method's accuracy. If nonfibrous background or interfering material is present to the extent that fibers are overlapped or covered up, the concentration of airborne fibers will be underestimated. Currently, NIOSH Method 7400 addresses this problem by stating that if more than 50% of the filter surface area is covered with particles, the

sample is overloaded and should be rejected as unacceptable for counting. The 50% filter surface coverage limit was intended as an upper limit and to a large extent, the decision of when to reject a sample was left up to the analyst. There is reason to believe that this recommended upper limit is inadequate for ensuring an accurate counting of fibers in all cases because factors that may have influenced the fiber counting efficiency may not have been taken into account.

Several studies have investigated the effect of loading on various aspects of fiber counting. One study calculated the decrease in count due to fiber-fiber overlap.⁽³⁾ Another preliminary study of the effect of loading indicated that the fiber count can be significantly affected at coverage levels of only 20%.⁽⁴⁾ A third study also indicated that significant undercounting can occur at relatively high levels of background dust

This work was funded by the Institute of Occupational Safety and Health, Council of Labor Affairs, Taiwan through grant IOSH-87-A103, and by a stipend for graduate education awarded by the National Taiwan University. Mention of company names or products does not constitute endorsement by the Centers for Disease Control and Prevention.

concentration.⁽⁵⁾ At low background dust concentrations, the opposite effect also may occur, namely, that fiber concentration is overestimated.⁽⁶⁾ However, the counting results obtained from applying the NIOSH Method 7400 "A" and "B" counting rules to determine fiber density were highly correlated.⁽⁷⁾ But essential information (such as the ratio of fiber number concentration to particle number concentration, resolution index, surface densities, and size distributions of fibers and particles) and their impact on the fiber counting efficiency have not been reported in a systematic and comprehensive manner in these studies.

A survey of analytical laboratories indicated that laboratories were inconsistent in their application of rejection criteria based on nonfibrous particle loading.⁽⁸⁾ The survey showed that some laboratories used the 50% coverage rule in Method 7400, whereas others used coverage as low as 20% to reject samples. Some labs rarely rejected samples for any reason. These survey results indicate the need for additional guidelines on the rejection of samples due to overloading. Thus, a computer simulation of the masking effect on fiber counting efficiency was carried out to examine the effects caused by various loading and size distribution parameters. Computer simulation was adopted for two reasons: (1) the exposure to hazardous fibrous particles is avoided, and (2) the ideal fiber generator capable of producing desired size distributions of fiber diameter and fiber length is not yet available.

It is likely that the fiber length and width distributions, the deposited particle density, the resolution of the observation system, the concentration ratio of fibrous to nonfibrous particles, and the counting method all affect the fiber counting efficiency. Therefore, one of the aims of this study was to estimate the bias introduced by various types of background dust at various dust concentrations and fiber concentrations. This information may help improve on the recommendations provided by NIOSH Method 7400 and deal better with such interferences. The main objectives of the present study were to establish the upper fiber and particle concentration limits for reliable counting and identification and to develop a method for correcting observed fiber counts for fibers not counted because of overlay or masking by other fibers or nonfibrous particles. The general approach to simulating fiber masking followed the technique by Chang et al. used for estimating bacterial colony counts affected by colony overlap.⁽⁹⁾

EXPERIMENTAL MATERIALS AND METHODS

Fibrous particles and nonfibrous particles will be referred to as fibers and particles, respectively. Prior to computer programming, the following assumptions were formed to facilitate computer simulation: (a) the fiber size (length and width) is a bivariate-lognormal distribution; (b) the fiber and particle positions in the graticule field are random; (c) the nonfibrous particles generated are spherical; and (d) the fiber shape is a rectangle with an aspect ratio greater than 5 (B rule of NIOSH method 7400). Fibers with an aspect ratio less than 5 were treated as nonfibrous particles. Some of the primary program input parameters were fiber count median length (CML), fiber count median width (CMW), geometric standard deviations (GSD) of fiber diameter and fiber length, resolution index (RI), number concentration ratio (fiber to particle), particle count median diameter (CMD) and particle GSD. The parameter ranges are shown in Table I.

A program written in Visual Basic® 4.0 (Microsoft, Redmond, Wash.) was used to simulate the fibers and particles on a graticule field (diameter 100 μm), which also was shown on the computer monitor to ensure proper execution of the program. The surface

TABLE I. Values of Parameters Used in Calculations

CML (μm)	CMW (μm)	Fiber GSD	RI	CR ^A	Particle CMD (μm)	Particle GSD
5	0.125	1.2	0.1	1:10	2	1.2
8	0.25	2	0.5	1:20	5	1.5
10	1	2.5	0.8	1:30	8	2
			0.9		10	3

^ACR: concentration ratio (fiber : particle)

areas of the graticule field, the fibers, and the particles were represented by regions on a Cartesian coordinate grid system. The choice of 2000 \times 2000 grid resolution was a compromise between accuracy and computation time, as shown in Figure 1. The difference between the "true fiber area" and the "area derived from the number of coordinate points within the boundaries of the fiber" was affected by the orientation of fiber, especially for the unique orientations, such as 0, 30, 45, or 90°. The fiber orientation was determined by using a seven-digit random number, so that the fiber was unlikely to have these unique orientations, which could have led to greater error. Running the whole list of all combinations, as shown in Table I, required 12 days on a Pentium 166 computer.

The difference between the observable area of a fiber under a phase contrast microscope (length 2 μm , width 0.125 μm) and the simulated area represented by the coordinate points inside the same rectangle was shown as a function of the resolution of the ordinate or abscissa axis (point/100 μm). The smallest diameter, 0.125 μm , was chosen to demonstrate the suitability of using discrete coordinate points to simulate the fiber areas. Figure 1 shows that the bias was less than 2%, assuming that the orientation of the fiber was not in any unique direction. Since the orientation was randomly produced by using a seven-digit fraction, such a unique orientation was highly unlikely to occur.

The RI is the fraction of a fiber that must be overlapped by the neighbor compact or fibrous particles before the fiber is counted. The RI was set at levels of 0.1, 0.5, 0.8, or 0.9 to indicate that the observation system was able to distinguish the fibers only

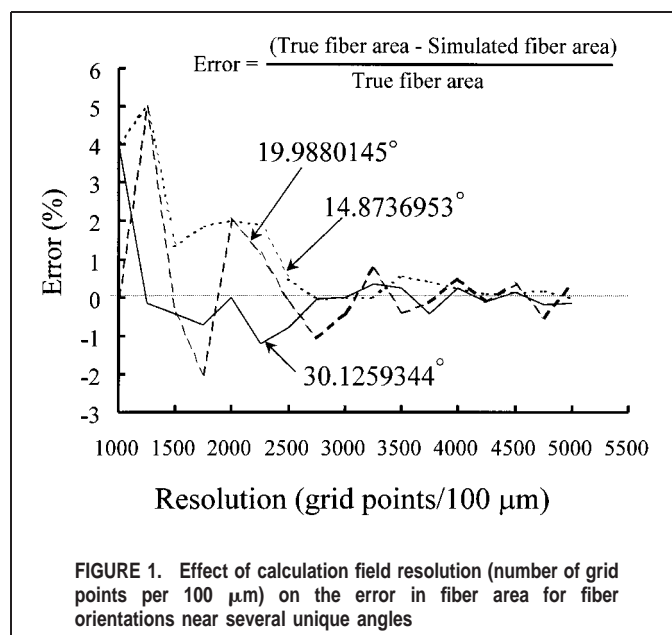


FIGURE 1. Effect of calculation field resolution (number of grid points per 100 μm) on the error in fiber area for fiber orientations near several unique angles

when the overlapped area of a fiber was equal to or less than 10, 50, 80, or 90% of the whole fiber, respectively. The fiber CML was set at 5, 8, or 10 μm . The CMW was 0.125, 0.25, or 1 μm from the detection limit of the phase contrast microscope to near the 50% cutoff size of 4 μm because the aerodynamic diameter of the fiber was about three times its physical diameter.⁽¹⁰⁾ The size distribution of fibers was set at GSDs of 1.5, 2.0, or 2.5. Due to the lack of published information, the simulated fiber-to-particle number concentration ratios were arbitrarily set at 1:10, 1:20, or 1:30. The CMD of coexisting particles was set at 2, 5, 8, or 10 μm . Unless the particle number concentration was extremely high, particles smaller than 2 μm were assumed to produce less of a masking effect on fiber counting because the cross-sectional area was much smaller. The particle GSD of 1.2 often was regarded by aerosol scientists as the upper limit for monodispersity.⁽¹¹⁾ In the present study GSDs ranging from 1.2 to 3.0 were included to simulate a wide range of conditions.

The size distribution parameters described above were applied to a simulated field as follows. The 100- μm diameter graticule field was placed in the first quadrant of a two-dimensional Cartesian coordinate system. The field diameter was divided into 2000 divisions. Therefore, there were 3,141,592 coordinate points representing the area of the observation field. Two random numbers were needed for each particle: one to determine the particle size and another to determine its location on the target field. For fiber simulation, four random numbers were needed for each fiber: (1) fiber length, (2) fiber width, (3) fiber location, and (4) fiber orientation. The coordinate points covered by a specific fiber or particle were then saved into a file. Once other fibers or particles overlapped this fiber or particle, the overlapping points were removed from the file. Then the preset resolution criteria were applied to determine the fiber counting efficiency. In the present study this process was repeated 20 times for each combination to increase statistical stability.

To accommodate those particles or fibers with a geometric center outside the border of the graticule field (i.e., with part of the fiber or particle still intruding the graticule field), the size of the fiber-particle generating field was defined as 1.4 times the diameter of the fiber counting field. Therefore, the fiber-particle generating field had a diameter of 140 μm . Assuming that the fiber CML was 10 μm (longer than the upper range of 8 μm simulated in the present study) and the GSD was 2, this fiber-particle generating field was estimated to include 97.5% of the simulated fibers. Thus, there was less than a 2.5% chance that the very long fibers located outside this fiber-particle generating field might extend into the graticule field.

The fibers were chosen to give a bivariate lognormal distribution:⁽¹²⁾

$$f(l, w) = \frac{1}{2\pi\beta_w\beta_L\sqrt{(1-\tau^2)/w}} \times \exp\left[-\frac{A^2 + B^2 - 2\tau AB}{2(1-\tau^2)}\right] \quad (1)$$

where

$$A = (\ln w - \mu_w)/\beta_w$$

$$B = (\ln l - \mu_L)/\beta_L$$

$$\tau = \frac{\beta_L\beta_w}{\beta_w\beta_L}$$

$$\beta_{lw} = \frac{1}{N-1} \sum_{i=1}^K \sum_{j=1}^M (\ln L_i - \mu_L)(\ln W_j - \mu_w)n_{ij}$$

μ_L = mean of fiber length, μ_w = mean of fiber width, $\beta_w^2 =$

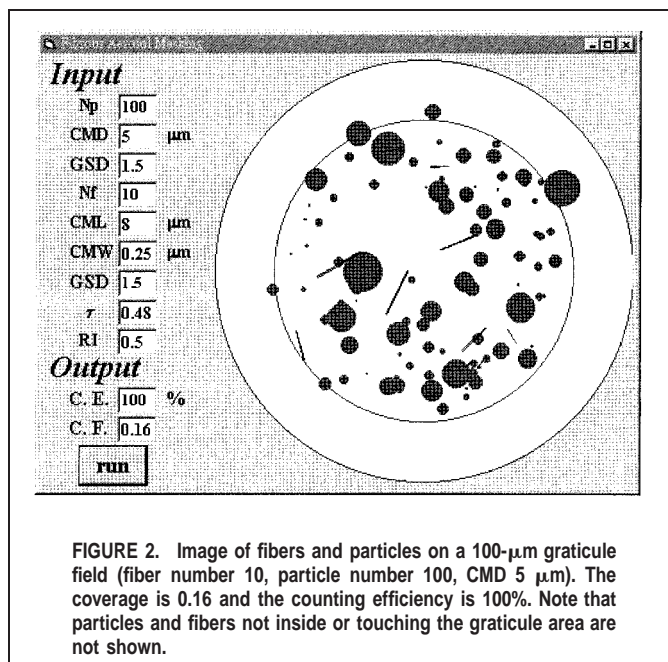


FIGURE 2. Image of fibers and particles on a 100- μm graticule field (fiber number 10, particle number 100, CMD 5 μm). The coverage is 0.16 and the counting efficiency is 100%. Note that particles and fibers not inside or touching the graticule area are not shown.

variation of fiber width, $\beta_L^2 =$ variation of fiber length, $\tau =$ correlation coefficient of fiber length and fiber width, $N =$ total fiber number, and $n_{ij} =$ number of fibers with length (L_i) and width (W_j). The correlation coefficient, τ , between the fiber length and fiber width was set at 0.48, as analyzed and reported in a study characterizing the size distribution of asbestos fiber aerosols.⁽¹²⁾

RESULTS AND DISCUSSION

To obtain a single case of masking, nine variables were specified. For example, in Figure 2 there were 100 particles (CMD = 5 μm and GSD = 1.5) and 10 fibers (CML = 8 μm , CMW = 0.25 μm , GSD = 1.5, and $\tau = 0.48$) generated within the fiber-particle generating field and counted within the graticule field with the preset RI of 0.5. For demonstration purposes, all the fibers in Figures 2–5 were shown whether they were on top or below the

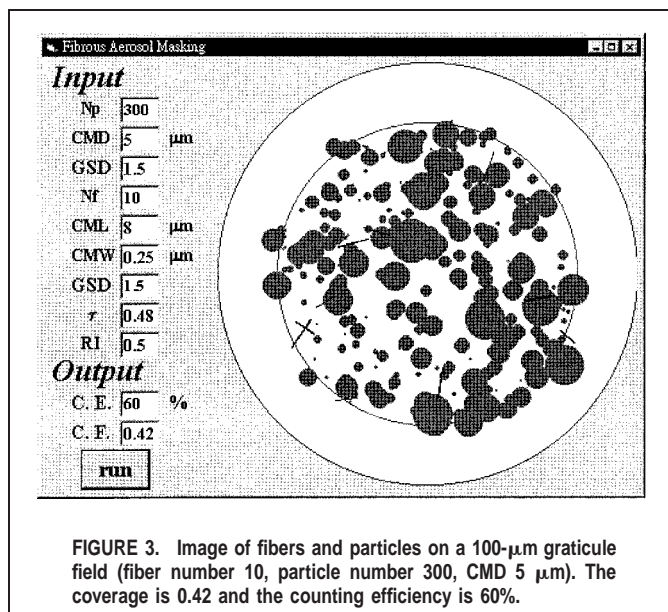
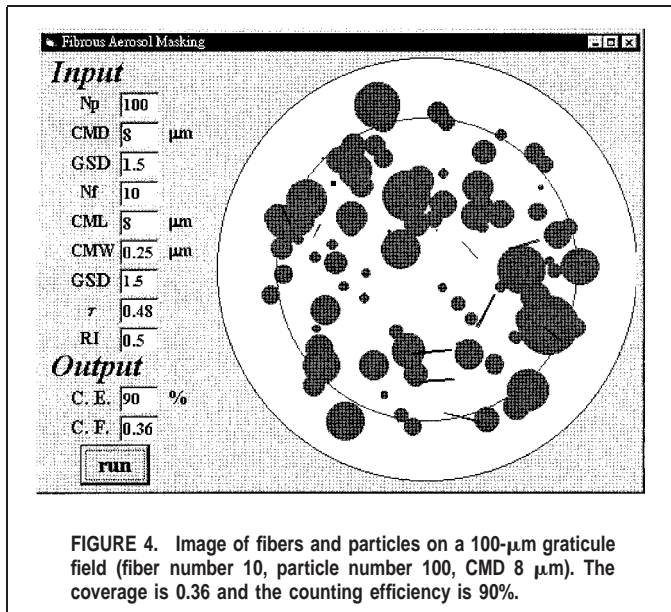


FIGURE 3. Image of fibers and particles on a 100- μm graticule field (fiber number 10, particle number 300, CMD 5 μm). The coverage is 0.42 and the counting efficiency is 60%.



particles. If a fiber was on top of the particles, it would be counted. These 100 particles and 10 fibers produced a coverage of 16% and a fiber counting efficiency of 100%. The variation in particle size was apparent because the GSD of 1.5 was greater than the limit for monodispersity (i.e., GSD = 1.2).

As the particle number increased from 100 (Figure 2) to 300 (Figure 3) and the rest of the parameters remained unchanged, the coverage increased from 0.16 to 0.42 and the counting efficiency decreased from 100 to 60%. Figure 3 explicitly showed that the higher number of particles caused the coverage to increase and resulted in a decreased counting efficiency. Notice that the fiber counting efficiency may not appear to be as high as 60% at first glance in Figure 3. This is because some of the fibers may sit on top of larger particle(s) because fibers and particles were generated in a random order. All fibers were shown to verify the total fiber number.

If the particle size was increased from 5 to 8 μm, as shown in Figure 4, 100 particles (CMD = 8 μm) contributed to as much

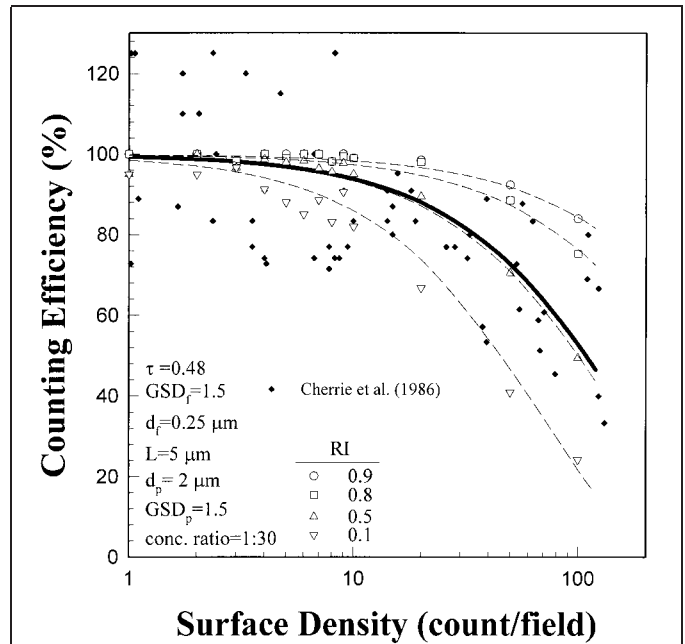
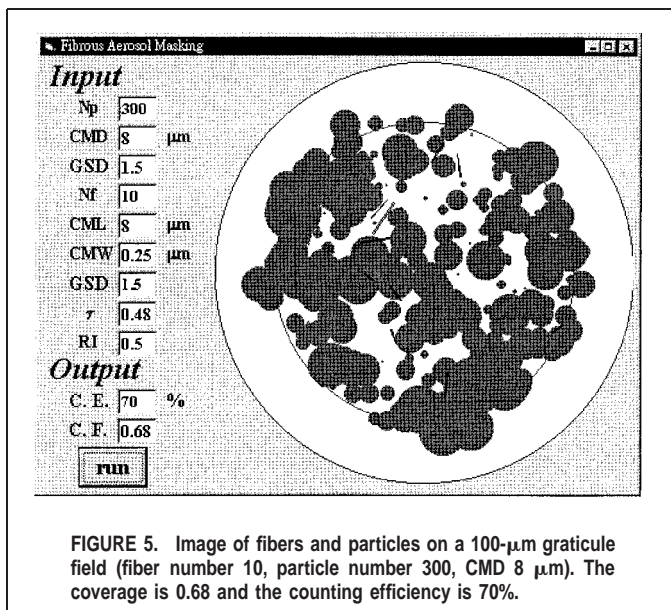
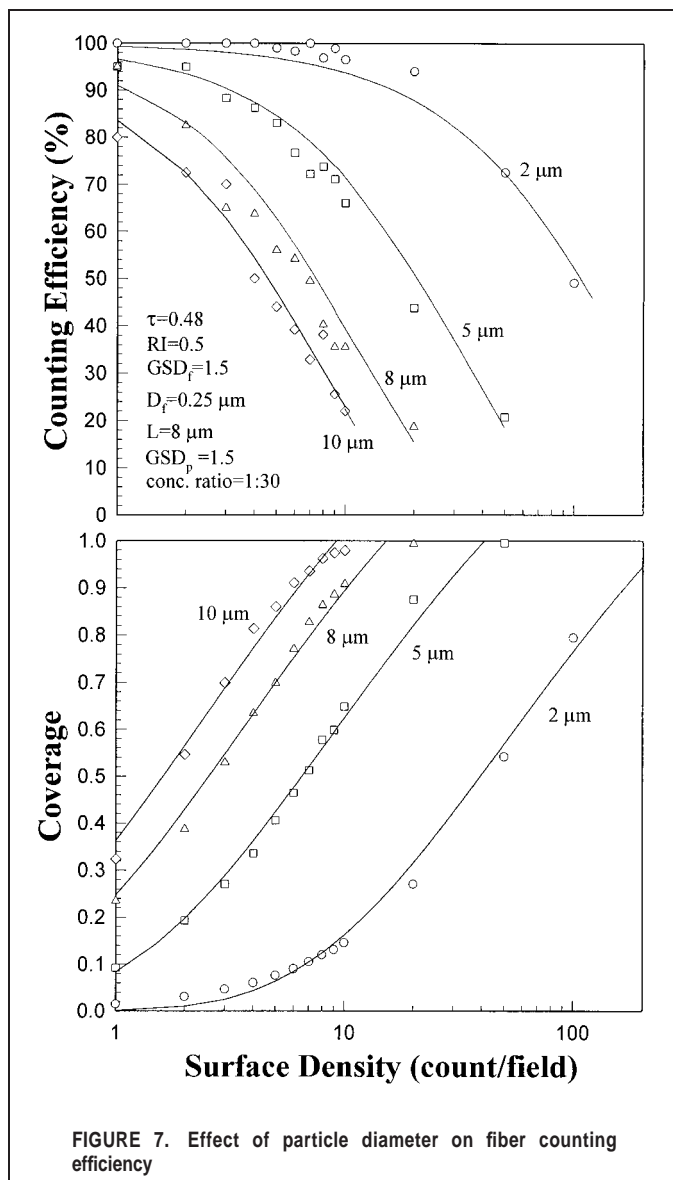


FIGURE 6. Estimation of resolution index of regression curve by Cherrie et al.⁽⁶⁾ assuming that the fiber-to-particle number concentration ratio is 1:30

coverage as 300 smaller particles (CMD = 5 μm), indicating that particle size was an important factor affecting the fiber counting efficiency. In the case of Figure 4 the counting efficiency dropped from 100% (of Figure 2) to 90%, with a coverage of 0.36. The fiber counting efficiency obtained by the simulation decreased with increasing coverage.

The heavy loading of a filter sample is demonstrated in Figure 5, in which the number of 8 μm particles increased from 100 (Figure 4) to 300. The coverage was 0.68, and the fiber counting efficiency dropped to 70%. This severe overlapping problem could be significantly alleviated if a preseparator such as a thoracic sampling device was used to remove particles larger than 10 μm aerodynamic diameter. The advantage of using a size-selective device is discussed in detail later in this article.

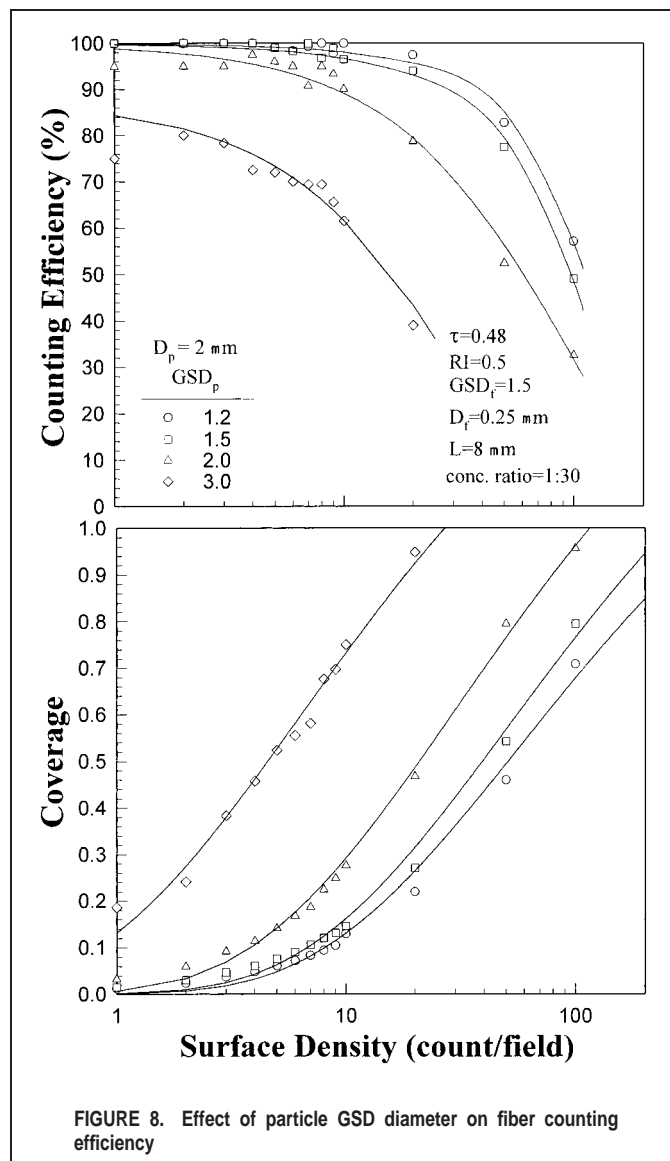
In previous studies^(5,6) fiber densities lower than 1000 fibers/mm² (equivalent to about 7.8 counts/field) were recommended to avoid bias due to the superposition of fibers either on other fibers or on particles. To evaluate the extent of underestimation as a function of fiber surface density, the published data points⁽⁶⁾ having surface density higher than 1 count/field were estimated and replotted to show the exponential decay, the best-fit bold solid line shown in Figure 6. Because of the lack of information on number concentration ratio of fiber to particle, the fiber-to-particle number concentration ratio was arbitrarily set at 1:30 to obtain an RI of approximately 0.5 during fiber counting by phase contrast microscopy. Notice that the counting efficiency curves derived from the computer simulation have the same general shape as the actual data. Figure 6 also shows that fiber counting efficiency was strongly dependent on the RI of the observing system, including the acuity of the counter. For the high RI of 0.9, the counting efficiency was never lower than 85%, even at the extremely high fiber density of 100 count/field and high fiber-to-particle concentration ratio. In contrast, the counting efficiency dropped from 85 to 20% when the RI decreased from 0.9 to 0.1. It is worth mentioning that the particle overlap may not be the



only factor influencing the actual counting efficiency, so comparison with actual data is needed.

Because the fiber number concentration was relatively low when compared with the particle number concentration coexisting in the atmospheric environment, the change in fiber length and width did not significantly alter the coverage of the microscopic field. Therefore, fiber counting efficiency remained approximately the same. For the same reason, the effect of fiber GSD on fiber counting efficiency also was negligible. In contrast, the size distribution of the nonfibrous particles (i.e., CMD and GSD) had a significant effect on fiber counting efficiency.

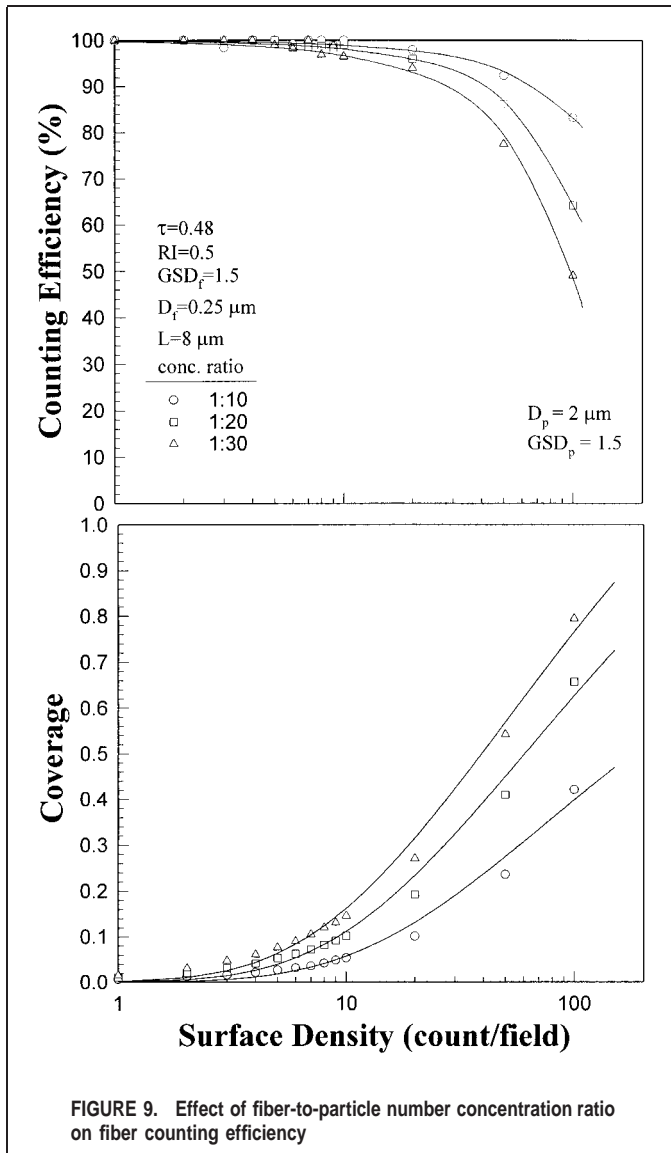
The effect of particle size on fiber counting efficiency is clearly demonstrated in Figure 7. The fiber CMW was set at 0.25 μm , fiber CML at 8 μm , fiber GSD at 1.5, RI at 0.5, τ at 0.48, particle GSD at 1.5, and fiber-to-particle concentration ratio at 1:30. The solid lines are the best-fit curves (with exponential terms) presenting the fiber counting efficiency and the coverage as a function of fiber surface density. As the fiber surface density increased, the coverage of the graticule field increased and the fiber counting efficiency exponentially decreased, as expected. Large particles tended to cover more of the graticule field given that the particle



number concentration and GSD remained the same and, therefore, caused the counting efficiency to drop more dramatically. For example, for the fiber density of 10 count/field, the coverages for 2, 5, 8, and 10 μm CMD particles were 0.14, 0.65, 0.91, and 0.98, respectively. The corresponding fiber counting efficiencies were 95, 71, 39, and 20%, respectively. The plots of counting efficiency curve happened to mirror the plots of the coverage curve, as shown in Figure 7.

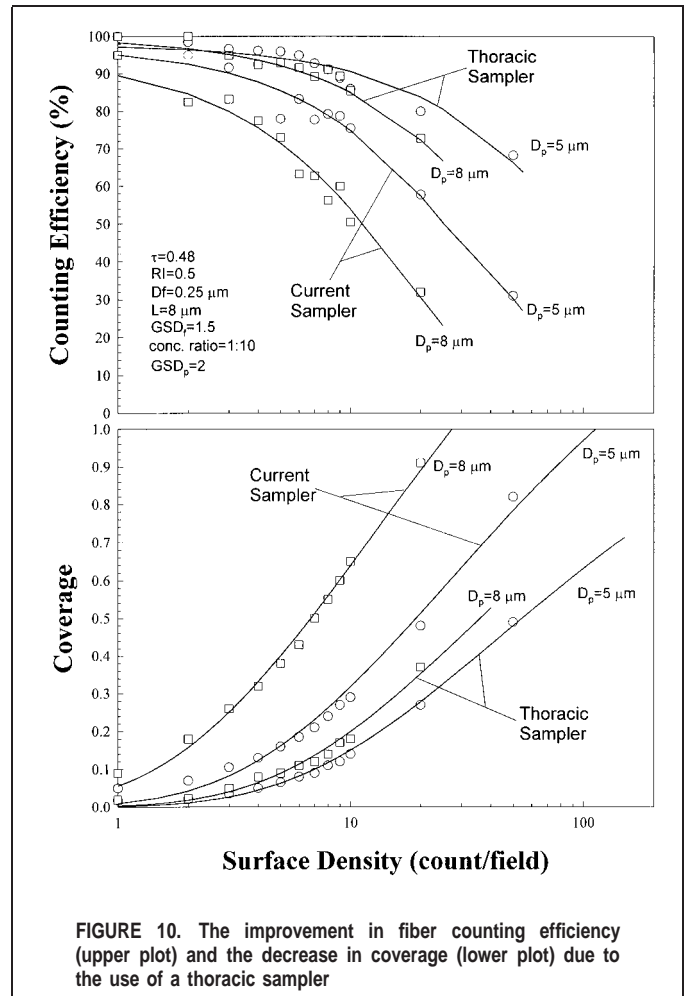
The effect of particle GSD on fiber counting efficiency and graticule field coverage was similar to that of particle size. Figure 8 shows that particles with higher GSDs tended to result in higher field coverage, and thus lower fiber counting efficiency. This mirrored plot of counting efficiency curve versus coverage curve indicates that as the GSD increases more large particles may cover more of the graticule field, and, thus, the likelihood of fibers to be counted may be reduced.

Based on the results of the studies by Iles and Johnston⁽⁵⁾ and Cherrie et al.,⁽⁵⁾ the NIOSH Method 7400 recommends that the upper fiber count limit not exceed 1300 count/ mm^2 , which is equivalent to about 10 counts/field. However, the fiber-to-particle number concentration ratio and the size distribution of the particles were not considered in these studies. The widely scattered



data points shown in Figure 6 were probably due to the lack of control in the fiber-to-particle number concentration ratio and the size distribution of the particles, in addition to the variability of the counting method. Intuitively, more particles would result in higher field coverage and, therefore, lower fiber counting efficiency, as shown in Figure 9. Again, the counting efficiency curve was a mirror of the coverage plot. The fiber-to-particle ratio could vary solely depending on the nature of the raw materials used or added during the manufacturing process (e.g., brake lining or asbestos cement). A pilot survey of a brake lining manufacturing plant (where chrysotile was used as the major ingredient) showed that the fiber-to-particle ratio was approximately 1:30 in the raw material blending area.

The purpose of air sampling and measurement is to obtain a representative sample that can be used to evaluate the health hazard of airborne particles in the workplace. To do so, comprehensive definitions of size-selective sampling have been defined because particles of different aerodynamic diameter are likely to deposit in different parts of the human respiratory tract.^(13,14) Asbestos fibers affect mainly the lungs, so the thoracic fraction appears most appropriate for sampling these fibers. However, in the contemporary practice of fiber sampling and measurement, there



is no device designed specifically to meet the thoracic size-selective criterion for fibers. The application of the thoracic sampling definition to fiber measurement was proposed in a previous study, which indicated that the current practice in many countries of counting only fibers having a diameter smaller than $3 \mu\text{m}$ diameter⁽¹⁵⁻¹⁷⁾ closely simulates the thoracic sampling definition.⁽¹⁸⁾ In the computer simulation the fibers and particles were classified using a thoracic penetration curve before placement on the graticule area. After removing the fibrous and nonfibrous particles larger than the 50% cutoff size of $10 \mu\text{m}$ the fiber counting efficiency could be significantly enhanced and field coverage reduced correspondingly, as shown in Figure 10. The fiber diameter was $0.25 \mu\text{m}$ with a fiber length of $8 \mu\text{m}$ and a GSD_f of 1.5, and fiber-to-particle ratio was set at 1:10. Assuming that the particle count median diameter was $8 \mu\text{m}$ with a GSD_p of 2, using a thoracic sampler could provide the benefit of an increase in counting efficiency from 62 to 92% because the field coverage would drop from 0.65 to 0.18. The improvement in fiber counting efficiency was less significant when the particle diameter was $5 \mu\text{m}$, that is, 82 to 94%. The improvement increased with increasing fiber density on the filter.

Kauffer and co-workers compared the data obtained using a porous-foam thoracic sampler with that from a standard French sampler.⁽¹⁹⁾ They showed that although significantly less particulate mass was collected using a thoracic sampler, the fiber count compared quite well with that obtained using the standard sampler.

This indicates that under optimal sampling conditions, the thoracic sampler will remove large particles from the sample, but will not affect the measured fiber concentration. The thoracic sampler also produced much better filter sample uniformity than the standard French asbestos sampler, which had an inlet much smaller (7 mm) than the filter diameter (47 mm). Further experimental work is needed to demonstrate improved performance using a thoracic sampler under various conditions of sample loading, especially at high dust concentrations.

CONCLUSIONS AND RECOMMENDATIONS

This computer simulation study focused largely on the problems of reduced fiber counting efficiency due to overlapping of fibers by other fibers or particles. The capability of distinguishing overlapped fibers (RI), the coverage of the graticule field, the fiber surface densities and size distribution of particles, and the fiber-to-particle concentration ratio all played significant roles in affecting the fiber counting efficiency. The fiber counting efficiency was found to decrease consistently with increasing surface density and decreasing RI. The recommended upper limit of fiber density on the membrane filter depended not only on the fiber surface density, as reported in previous studies, but also on the fiber-to-particle number concentration ratio and the size distributions of fibers and particles.

When the fiber number concentration in the workplace is lower than the particle number concentration, then the change in fiber size distribution (CMW, CML, GSD) will not readily affect the coverage of the graticule field, and, thus, the fiber counting efficiency will remain unchanged. In contrast, particle size and distribution are more likely to have a significant impact on the graticule field coverage and thus the fiber counting efficiency.

The advantage of using a thoracic preseparator is significant, especially when the particle CMD is close to or larger than the thoracic cutoff size of 10 μm . The improvement in fiber counting efficiency is expected to become more prominent as the fiber-to-particle number concentration increases. However, in addition to the fit to the thoracic convention, the fiber measurement method further requires that the fiber sample be uniformly deposited on the membrane filter.

REFERENCES

1. National Institute for Occupational Safety and Health (NIOSH): Fibers, Method 7400 Issue #2 (8/15/94). In *NIOSH Manual of Analytical Methods*. Cincinnati, Ohio: NIOSH, 1994.
2. "Asbestos-containing materials in schools." *Final Rule* (52 FR 41826), Oct. 30, 1987.
3. Knight, G.: Overlap problems in counting fibers. *Am. Ind. Hyg. Assoc. J.* 36:113-114 (1975).
4. Peck, A.S., J.J. Serocki, and L.C. Dicker: Sample density and the quantitative capabilities of PCM analysis for the measurement of airborne asbestos. *Am. Ind. Hyg. Assoc. J.* 47:A230-A234 (1986).
5. Iles, P.J., and A.M. Johnston: Problems of asbestos fibre counting in the presence of fibre-fibre and particle-fibre overlap. *Ann. Occ. Hyg.* 27:389-403 (1983).
6. Cherie, J., A.D. Jones, and A.M. Johnston: The influence of fiber density on the assessment of fiber concentration using the membrane filter method. *Am. Ind. Hyg. Assoc. J.* 47:465-474 (1986).
7. Buchta, T.M., C.H. Rice, J.E. Lockey, G.K. Lemasters, and P.S. Gartside: A comparative study of the National Institute for Occupational Safety and Health 7400 "A" and "B" counting rules using refractory ceramic fibers. *Appl. Occup. Environ. Hyg.* 13:58-61 (1998).
8. Marshall, C.P.: PCM rejection policies differ. *Asbestos Issues* 3(10): 16-18 (1990).
9. Chang, C.W., Y.-H. Hwang, S.A. Grinshpun, J.M. Macher, and K. Willeke: Evaluation of counting error due to colony masking in bioaerosol sampling. *Appl. Environ. Microbiol.* 60:3732-3738 (1994).
10. Chen, C.-C., and P.A. Baron: Aspiration efficiency and wall deposition in the fiber sampling cassette. *Am. Ind. Hyg. Assoc. J.* 52:142-152 (1996).
11. John, W.: The characteristics of environmental and laboratory-generated aerosols. In K. Willeke and P.A. Baron, editors, *Aerosol Measurement*, pp. 54-76. New York: Van Nostrand Reinhold, 1993.
12. Cheng, Y.-S.: Bivariate lognormal distribution for characterizing asbestos fiber aerosols. *Aerosol Sci. Technol.* 5:359-368 (1986).
13. American Conference of Governmental Industrial Hygienists. Appendix D: Particle size-selective sampling criteria for airborne particulate matter. In *1997 TLVs and BEIs*. pp. 47-50. Cincinnati, Ohio: American Conference of Governmental Industrial Hygienists, 1997.
14. International Standards Organization (ISO): *Air Quality-Particle Size Fraction Definitions for Health-Related Sampling* [TR 7708: 1995(E)]. Geneva: ISO, 1995.
15. International Standards Organization (ISO): *Determination of Airborne Inorganic Fibre Concentrations in Workplaces by Light Microscopy (Membrane Filter Method)*. Geneva: ISO, 1982.
16. World Health Organization (WHO): *Determination of Airborne Fibre Number Concentrations: A Recommended Method by Phase Contrast Optical Microscopy (Membrane Filter Method)*. Geneva: WHO, 1997.
17. Health and Safety Executive: *MDHS 39/3 Asbestos Fibres in Air* (MDHS 39/3). London: Health and Safety Executive, 1990.
18. Baron, P.A.: Application of the thoracic sampling definition to fiber measurement. *Am. Ind. Hyg. Assoc. J.* 57:820-824 (1996).
19. Kauffer, E., J.C. Vigneron, J. Fabriés, M.A. Billon-Galland, and P. Brochard: The use of a new static device based on the collection of the thoracic fraction for the assessment of the airborne concentration of asbestos fibres by transmission electron microscopy. *Ann. Occup. Hyg.* 40:311-319 (1996).